Check for updates

LASER & PHOTONICS REVIEWS
www.lpr-journal.org

Experimental Preparation of Optical Cat States Carrying Orbital Angular Momentum

*Chenyu Qiao, Fengyi Xu, Meihong Wang, Rong Ma, and Xiaolong Su**

As an important quantum resource, optical cat state is successfully prepared and applied in quantum information science. It is shown that optical quantum states carrying orbital angular momentum (OAM) have wide applications in quantum communication and quantum precision measurement. Here, optical cat states carrying OAM are experimentally prepared with topological charges $\ell = 0, +1, +2, +4$ by changing the wavefront of the photon-subtracted squeezed vacuum state with a combination of quarter-wave plate and q-plate. To verify the prepared cat states, both Wigner functions and topological charges of OAM are measured. It is shown that the fidelities and amplitudes of optical cat states carrying OAM decrease slightly with the increase of topological charges of OAM, although the spatial size of the optical beam is increased. These results present a new kind of optical cat state carrying OAM, which has potential applications in quantum precision measurement.

1. Introduction

Schrödinger cat state, as a typical superposition state,[1] has been identified as an important quantum resource in both quantum information[2–8] and quantum precision measurement.[9,10] Optical cat state, which is the superposition of two coherent states $|\alpha\rangle$ and $|-\alpha\rangle$, has attracted much attention in quantum information processing due to the weak interaction with the environment.[3–6] By subtracting photons from squeezed vacuum states,[11,12] optical cat states with $\alpha \sim 1$ have been experimentally prepared.[13,14] In addition, large-amplitude optical cat states are generated by the techniques of ancilla-assisted photon subtraction[15] and subtracting three photons from a squeezed vacuum state.[16] The preparation of an optical cat state combines the Gaussian resource and the photon counting technique, which is a typical hybrid continuous- and discrete-variable quantum information processing.[17–19] Recently, remote preparation of optical cat states based on the Gaussian entangled state[20] and the quantification of quantum coherence of optical cat states in a lossy channel[21] have been also demonstrated. Furthermore, squeezed cat state has also been experimentally prepared,[22–26] since it has potential application in quantum error correction[8] and slowing the decoherence of optical cat states.[26–28] For the applications of optical cat states, quantum teleportation of cat states,[29] tele-amplification,[30] preparation of hybrid entangled states,[31–34] and the Hadamard gate[35] have been demonstrated experimentally based on prepared optical cat states. Besides the applications in quantum information, optical cat states have potential applications in improving the sensitivity of quantum precision measurement.[9,10]

It has been shown that the multimode spatial structure of the quantum state is helpful in enhancing the performance of quantum precision measurement. Orbital angular momentum (OAM) of light with the transverse spatial distribution, which is a special degree of freedom, has been applied in multiparameter estimation,[36] rotating-angle measurements,[37] rotating-speed measurements,[38,39] ultra-sensitive and superresolution angular measurement,[40,41] and the improvement of angular resolution of remote sensing.[42,43] Up to now, discrete-variable quantum resources carrying OAM, such as NOON state,[40] two-photon[43,44] and multi-photon quantum entanglement,[45,46] multipartite quantum entanglement and quantum steering,[47] have been generated successfully. In the continuous-variable system, the OAM degree of freedom has been introduced to twin beam,[48] bipartite entangled state,[49–51] hyperentanglement,[52] multipartite entangled state[53,54] and quantum steering.[55] Moreover, because the characterization of inherent high dimensions is helpful to increase the channel capacity in quantum communication,[56] quantum resource carrying OAM has also been applied in performing quantum teleportation,[57–59] quantum dense coding,[60] building quantum networks,[61,62] and constructing a quantum memory.[63]

In the previous experiments, the transverse spatial distribution of optical cat states are limited to the TEM_{00} Gaussian beam, where the OAM degree of freedom is not introduced. Inspired by the potential application of both optical cat state and OAM of light in quantum precision measurement, it is essential to prepare the optical cat state carrying OAM degree of freedom, which may further improve the precision of quantum measurement. For example, it has been shown that higher sensitivity and resolution in phase estimation could be achieved by combining OAM

C. Qiao, F. Xu, M. Wang, R. Ma, X. Su
State Key Laboratory of Quantum Optics and Quantum Optics Devices
Institute of Opto-Electronics
Shanxi University
Taiyuan 030006, China
E-mail: suxl@sxu.edu.cn
M. Wang, R. Ma, X. Su
Collaborative Innovation Center of Extreme Optics
Shanxi University
Taiyuan, Shanxi 030006, China

The ORCID identification number(s) for the author(s) of this article can be found under https://doi.org/10.1002/lpor.202400174

DOI: 10.1002/lpor.202400174

 © 2024 Wiley-VCH GmbH

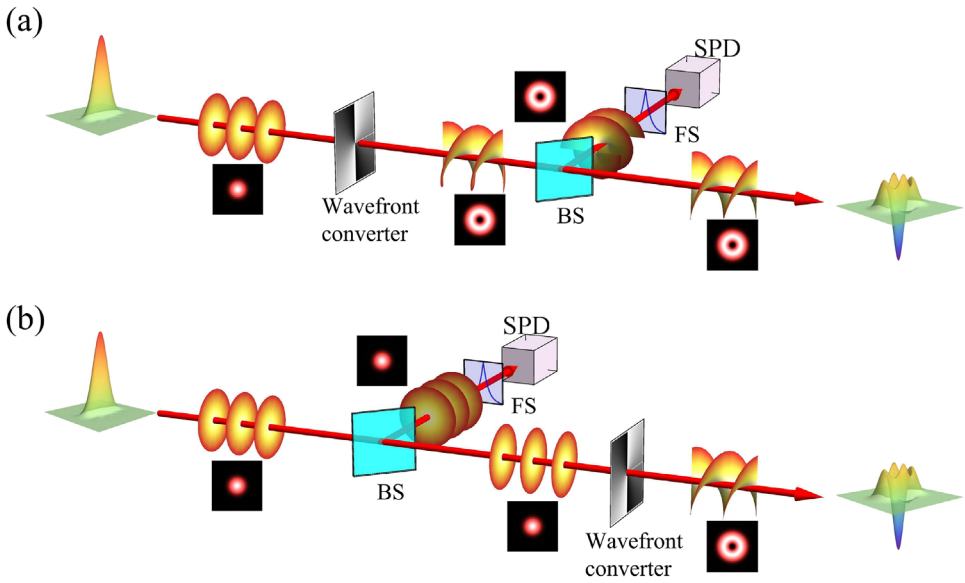

Figure 1. Principles of two methods to prepare optical cat states carrying OAM. a) The optical cat state carrying OAM is prepared by subtracting a photon from a squeezed vacuum state carrying OAM. b) The optical cat state carrying OAM is prepared directly by changing the spatial distribution of the photon-subtracted squeezed vacuum state. The filter system is used to filter out the nondegenerate mode of the squeezed vacuum state, and make sure the degenerate modes reach the SPD. BS, the beam splitter used for photon subtraction; FS, filter system; SPD, single photon detector.

and non-Gaussian states.[41,64] Although an analogous cat state encoded in OAM space is simulated by engineering the classical OAM of light,[65] the preparation of the optical cat state carrying OAM by subtracting photons from a squeezed vacuum state still remains a challenge.

Here, we experimentally prepare optical cat states carrying OAM by introducing OAM degree of freedom into the preparation system of the cat state directly. We propose two methods to prepare optical cat states carrying OAM, where a wavefront converter is used to convert the spatial distribution of the squeezed vacuum state before photon subtraction or that of photon-subtracted squeezed vacuum state respectively. In the experiment, optical cat states carrying OAM with $\ell = 0, +1, +2, +4$ are obtained by converting the photon-subtracted squeezed vacuum state with a combination of quarter-wave plate (QWP) and q-plate. The measured Wigner functions of output states and the topological charges of OAM confirm the successful preparation of cat states carrying OAM. Our work extends the degree of freedom of optical cat states by introducing OAM, which may have potential application in high-precision quantum measurement.

2. The Principle

The optical cat state carrying Laguerre-Gaussian (LG) mode is described as

$$|\Psi_{LC}\rangle_{\ell,p} = \frac{1}{\sqrt{2(1+cos\phi e^{-2|\alpha|^2})}}(|\alpha\rangle_{\ell,p} + e^{i\phi}|-\alpha\rangle_{\ell,p}) \quad (1)$$

where the subscripts of ℓ and p denote the azimuthal and radial index of the LG mode, and the cat state is an even or odd cat state in case of $\phi = 0$ or $\phi = \pi$. Each LG mode with $\ell \neq 0$ carries a quantized OAM $\ell\hbar$ and we refer to LG modes with $p = 0$ as OAM.[66–68] Thus, the optical odd cat state carrying OAM is given by

$$|\Psi_{LC}\rangle_{\ell} = \frac{1}{\sqrt{2(1-e^{-2|\alpha|^2})}}(|\alpha\rangle_{\ell} - |-\alpha\rangle_{\ell}) \quad (2)$$

We propose two methods to prepare optical odd cat states carrying OAM shown in Equation (2). As shown in **Figure 1**, a Gaussian beam is converted to a vortex beam by a wavefront converter,[56] which transforms the planar wavefront into a helical wavefront $\exp(i\ell\theta)$, where θ is the angular coordinate. In the first method shown in Figure 1a, an optical cat state carrying OAM is prepared by subtracting a photon from a squeezed state carrying OAM. A squeezed vacuum state with $\ell = 0$ is converted into a squeezed state carrying OAM first by a wavefront converter, then a photon is subtracted. The challenges of this method are that the filter system needs to be updated to filter out the nondegenerate modes carrying OAM, which is less efficient than the normal Gaussian mode ($\ell = 0$), and the generation rate of the optical cat state carrying OAM may decrease.

In the second method shown in Figure 1b, by subtracting a photon from squeezed vacuum state with planar wavefront, the photon-subtracted squeezed vacuum state (approximate optical cat state) with planar wavefront is prepared first. Then, the photon-subtracted squeezed vacuum state with $\ell = 0$ is converted into an optical cat state carrying OAM by a wavefront converter. When there is a click on the single photon detector (SPD), a cat state carrying OAM is prepared successfully. Compared to the first method, the advantages of the second method are embodied in two aspects. At first, it is more convenient for the second method, since the filter system before SPD does not need to be updated for corresponding OAM modes. Second, the generation rates of cat states carrying OAM of the second method

© 2024 Wiley-VCH GmbH

18638899, 0, Downloaded from https://onlinelibrary.wiley.com/doi/10.1002/lpor.202400174 by Shanxi University, Wiley Online Library on [14/10/2024]. See the Terms and Conditions (https://onlinelibrary.wiley.com/terms-and-conditions) on Wiley Online Library for rules of use; OA articles are governed by the applicable Creative Commons License

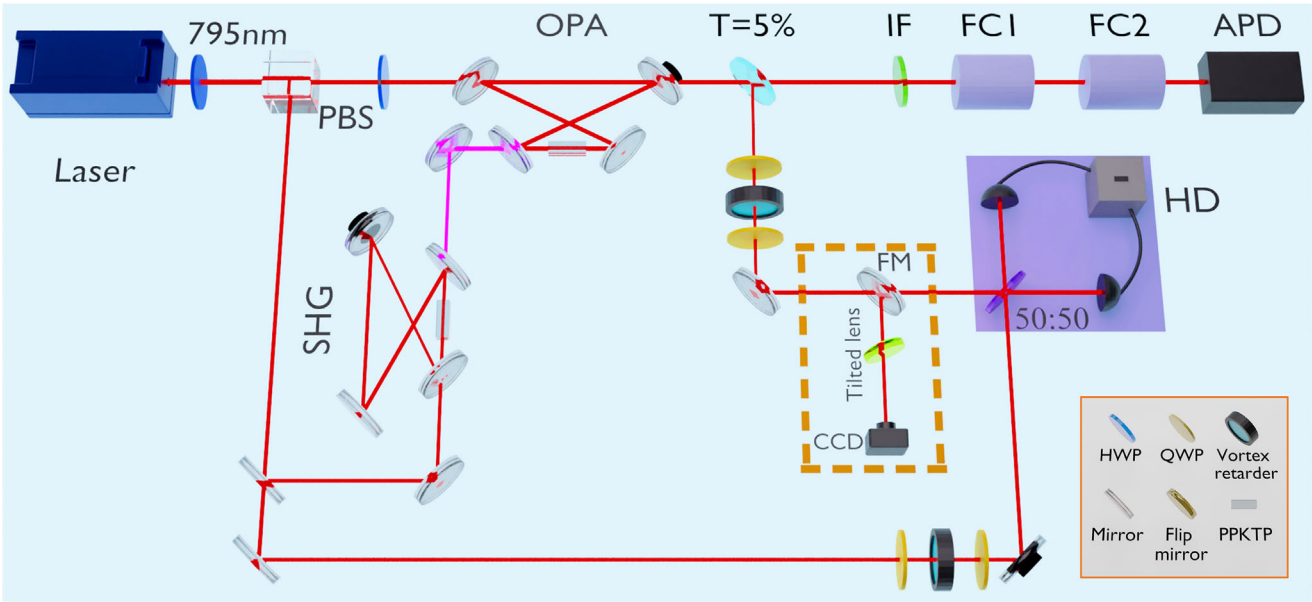

Figure 2. Experimental setup of preparing optical cat states carrying OAM. A photon click in APD heralds photon subtraction from the squeezed vacuum state, which is realized by the beam-splitter with a transmittance of $T = 5\%$. The wavefront converter consists of two QWPs and a q-plate (vortex retarder). SHG, second harmonic generator; HWP, half-wave plate; QWP, quarter-wave plate; PBS, polarization beam splitter; OPA, optical parametric amplifier; IF, interference filter with 0.4 nm bandwidth; FC, filter cavity; FM, flip mirror; LO, local oscillator; APD, avalanche photodiode; HD, homodyne detector.

remain the same as the cat state in Gaussian mode. Thus, we choose the second method to prepare the optical cat states carrying OAM in our experiment.

3. Experimental Section

As shown in **Figure 2**, a continuous wave single frequency Ti: Sapphire laser operated at 795 nm, corresponding to the rubidium D1 line, was used as a light source. The laser beam was split into three parts, which serve as the input beam of the second harmonic generation (SHG), the seed beam of the optical parametric amplifier (OPA), and local oscillator for the homodyne detector (HD), respectively. The output beam at 397.5 nm from the SHG was used as the pump beam of the OPA. A squeezed vacuum state with −3 dB squeezing was generated by the OPA which contains a periodically poled $KTiOPO_4$ (PPKTP) crystal with a pump power of 25 mW. By subtracting a photon from the squeezed vacuum state through a beam-splitter with a transmissivity of 5%, an odd optical cat state with $\ell = 0$ was experimentally prepared when a photon was detected by an avalanche photodiode (APD). To pick out the degenerate longitudinal mode same to that detected by the HD, the subtracted photon passes through a filter system, which consists of an interference filter with 0.4 nm bandwidth and two filter cavities with fineness of 1200, whose cavity lengths are 0.75 and 2.05 mm respectively. After the filter system, an isolation ratio with −30 dB (0.1% rejection) for the nondegenerate modes was obtained.

To generate the OAM modes, a wavefront converter containing two QWPs and a q-plate (vortex retarder)[69,70] with the transmittance of 98%, which only introduces 2% loss, was inserted in the path of the photon-subtracted squeezed vacuum state. In the wavefront converter, the linear polarization of a Gaussian beam was turned into left (right) circular polarization by the first QWP. Then, a vortex beam with the topological charge of $+\ell$ $(-\ell)$ was obtained after a q-plate and the left (right) circular polarization is turned into the right (left) circular polarization. Finally, the right (left) circular polarization of the output beam of the q-plate was turned into linear polarization by the second QWP to satisfy the requirement of HD. In this way, the optical cat state carrying OAM with topological charge $+\ell$ $(-\ell)$ was obtained.

In order to characterize the generated cat states carrying OAM, both Wigner functions and topological charges of output states were measured. At first, quantum tomography was performed to reconstruct the Wigner function of the cat state based on the output of the homodyne detector.[71] In the homodyne measurement, the local oscillator carrying OAM with the opposite topological charge as the cat state was needed, which was obtained by inserting the same order wavefront converter into the path of the local oscillator. Fifty thousand photocurrents were taken from the homodyne detector to obtain the density matrix in Fock basis with a photon number cutoff of 11 using the maximum-likelihood algorithm.[71] According to the obtained density matrix, the Wigner function of the cat state carrying OAM was reconstructed.

Second, both spatial distributions and topological charges of the prepared cat states were measured with the experimental setup shown in the dashed box of Figure 2 to verify the properties of OAM. After the wavefront converter, the vortex beam carrying OAM was reflected twice, and then enters into a CCD camera to record its spatial distribution. In order to identify the topological charge of the cat state, a tilted lens with $R = 70$ mm was inserted in front of the CCD camera. A transverse intensity profile with symmetric interference-like patterns, which characterizes the information of topological charge, was recorded by the CCD camera.

© 2024 Wiley-VCH GmbH

18638899, 0, Downloaded from https://onlinelibrary.wiley.com/doi/10.1002/lpor.202400174 by Shanxi University, Wiley Online Library on [14/10/2024]. See the Terms and Conditions (https://onlinelibrary.wiley.com/terms-and-conditions) on Wiley Online Library for rules of use; OA articles are governed by the applicable Creative Commons License

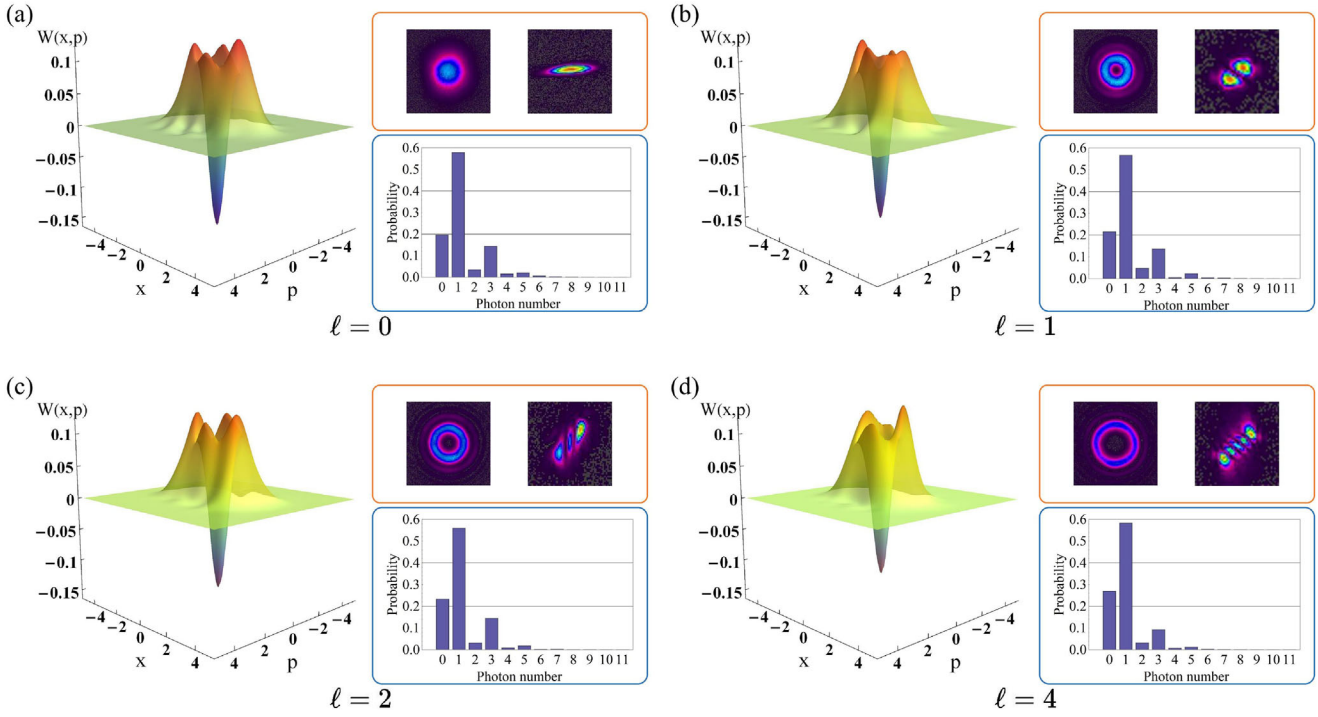

Figure 3. Experimental results of cat states with different topological charges. a–d), Wigner functions of cat states carrying topological charges with $\ell = 0, +1, +2, +4$, respectively, which are corrected with the corresponding detection efficiencies shown in Table 1. Left and right pictures in the orange insets, spatial and intensity distributions of prepared cat states carrying OAM; the blue insets, the photon number distributions of the cat states carrying OAM.

4. The Results

The reconstructed Wigner functions of prepared cat states carrying OAM with $\ell = 0, +1, +2, +4$, are shown in **Figure** 3a–d, respectively. Optical cat states with center negative dip $W(0,0) = -0.16 \pm 0.003$, -0.15 ± 0.003, -0.14 ± 0.004, -0.12 ± 0.005 are obtained for topological charges $\ell = 0, +1, +2, +4$, respectively. Comparing the Wigner functions of cat states with nonzero topological charge ($\ell \neq 0$) shown in Figure 3b-d with that of $\ell = 0$ Figure 3a, it is obvious that the properties of the prepared cat states carrying OAM do not change dramatically with the increase of topological charges of OAM.

The measured spatial distributions and intensity distributions with symmetric interference-like patterns of the cat states carrying OAM with different topological charges are shown in the orange insets in Figure 3. Comparing the spatial distribution of OAM shown in the left pictures of the orange insets, we show that the beam size of the cat states increases with the increase of topological charges. Based on the measured intensity distributions with symmetric interference-like patterns shown in the right pictures of the orange insets, we confirm that the cat states carrying OAM with $\ell = 0, +1, +2, +4$ are obtained, where the sign and magnitude of the topological charge of OAM are determined by the orientation of the stripes and the number of the bright stripes n with the relation of $|\ell| = n - 1$, respectively.[72]

To quantify the quality of prepared cat states carrying OAM, we calculate the fidelity

$$F_\ell = {}_\ell\langle \Psi_{LC} | \hat{\rho}_\ell^{out} | \Psi_{LC} \rangle_\ell \quad (3)$$

Table 1. Experimental results of different topological charges.

Topological charge	Amplitude	Fidelity	Negativity	Visibility	Detection efficiency
0	1.05 ± 0.01	0.69 ± 0.01	-0.16 ± 0.003	98.5%	80%
+1	1.01 ± 0.02	0.67 ± 0.01	-0.15 ± 0.003	98%	79%
+2	1.03 ± 0.01	0.66 ± 0.01	-0.14 ± 0.004	97%	78%
+4	0.90 ± 0.03	0.65 ± 0.02	-0.12 ± 0.005	95%	75%

which is defined as the overlap between an ideal odd cat state carrying OAM $|\Psi_{LC}\rangle_\ell$ and the experimentally reconstructed quantum state $\hat{\rho}_\ell^{out}$. In the case of $\ell = 0$, an approximate optical cat state with amplitude of $\alpha_0 = 1.05 \pm 0.01$ is experimentally obtained with the fidelity of $F_0 = 0.69 \pm 0.01$. When the topological charge of the OAM increases to $\ell = +4$, an optical cat state with the fidelity of $F_4 = 0.65 \pm 0.02$ and amplitude of $\alpha_4 = 0.9 \pm 0.03$ is experimentally prepared. The details of the experimental results are listed in **Table** 1. All these results confirm the successful generation of optical cat states carrying different OAM. The generation rates of the cat states carrying different OAM are all ≈ 2 kHz, which are the same as that of the cat state with $\ell = 0$.

In principle, the fidelity, amplitude, and negativity of prepared cat states carrying different topological charges should be identical. Comparing the results of cat states carrying OAM with different topological charges in Table 1, we show that the amplitudes and fidelities of the prepared OAM cat states only decrease slightly with the increase of topological charges. This is because

© 2024 Wiley-VCH GmbH

18638899, 0, Downloaded from https://onlinelibrary.wiley.com/doi/10.1002/lpor.202400174 by Shanxi University, Wiley Online Library on [14/10/2024]. See the Terms and Conditions (https://onlinelibrary.wiley.com/terms-and-conditions) on Wiley Online Library for rules of use; OA articles are governed by the applicable Creative Commons License

the visibilities and detection efficiencies between signal and local oscillator of the homodyne detector decrease slightly with the increase of the beam size, which may be improved by an OAM shaped local oscillator.[73]

5. Discussion and Conclusion

In our experiment, optical cat states carrying OAM with a fixed topological charge are prepared, which are limited by the property of the q-plate. By combining the non-Gaussianity of cat states and OAM in quantum precision measurement,[64] cat states carrying OAM may be applied to improve the precision of quantum measurement. More importantly, OAM multiplexed quantum states have more advantages than quantum states carrying a fixed OAM since more OAM degrees of freedom are involved. In order to prepare the OAM multiplexed cat states, a spatial light modulator, instead of a q-plate, should be used. Furthermore, it is interesting to prepare cat states with variously spatial distributions, such as Hermite-Gaussian mode,[36] Laguerre-Gaussian mode,[37] and hypergeometric-Gaussian mode.[69,70] And it is worthwhile to extend the applications of cat states carrying OAM.

In summary, we propose two methods to prepare cat states carrying OAM, which are subtracting photons from the squeezed vacuum state carrying OAM and converting the photon-subtracted squeezed vacuum state with $\ell = 0$ into the cat state carrying OAM by a wavefront converter, respectively. In our experiment, we successfully prepare optical cat states carrying OAM with $\ell = 0, +1, +2, +4$ respectively by inserting a combination of QWP and q-plate on the path of the photon-subtracted squeezed vacuum state. The prepared cat states carrying different OAM are confirmed by the measured Wigner functions and topological charges of OAM. Comparing the Wigner functions of cat states carrying different OAM, we show that the fidelities, amplitudes, and negativities decrease slightly with the increase of the topological charges of OAM. Our work demonstrates the feasibility of preparing cat states carrying OAM, which introduces a new degree of freedom to optical cat states, and provides a quantum resource for quantum-enhanced precision measurement with cat states carrying OAM.

Acknowledgements

This research was supported by the NSFC (Grant No. 11834010), Fundamental Research Program of Shanxi Province (Grant No. 20210302121002), and Fund for Shanxi "1331 Project" Key Subjects Construction.

Conflict of Interest

The authors declare no conflict of interest.

Data Availability Statement

The data that support the findings of this study are available from the corresponding author upon reasonable request.

Keywords

cat state, orbital angular momentum, photon subtraction, squeezed state

Received: February 2, 2024
Revised: June 11, 2024
Published online:

[1] E. Schrödinger, *Naturwissenschaften* **1935**, *23*, 807.
[2] M. Arndt, K. Hornberger, *Nat. Phys.* **2014**, *10*, 271.
[3] S. J. van Enk, O. Hirota, *Phys. Rev. A* **2001**, *64*, 022313.
[4] H. Jeong, M. S. Kim, *Phys. Rev. A* **2002**, *65*, 042305.
[5] T. C. Ralph, A. Gilchrist, G. J. Milburn, W. J. Munro, S. Glancy, *Phys. Rev. A* **2003**, *68*, 042319.
[6] A. P. Lund, T. C. Ralph, H. L. Haselgrove, *Phys. Rev. Lett.* **2008**, *100*, 030503.
[7] B. Hacker, S. Welte, S. Daiss, A. Shaukat, S. Ritter, L. Li, G. Rempe, *Nat. Photonics* **2019**, *13*, 110.
[8] D. S. Schlegel, F. Minganti, V. Savona, *Phys. Rev. A* **2022**, *106*, 022431.
[9] J. Joo, W. J. Munro, T. P. Spiller, *Phys. Rev. Lett.* **2011**, *107*, 083601.
[10] A. Gilchrist, K. Nemoto, W. J. Munro, T. C. Ralph, S. Glancy, S. L. Braunstein, G. J. Milburn, *J. Opt. B: Quantum Semiclassical Opt.* **2004**, *6*, S828.
[11] M. Dakna, T. Anhut, T. Opatrný, L. Knöll, D.-G. Welsch, *Phys. Rev. A* **1997**, *55*, 3184.
[12] A. P. Lund, H. Jeong, T. C. Ralph, M. S. Kim, *Phys. Rev. A* **2004**, *70*, 020101(R).
[13] A. Ourjoumtsev, R. Tualle-Brouri, J. Laurat, P. Grangier, *Science* **2006**, *312*, 83.
[14] J. S. Neergaard-Nielsen, B. M. Nielsen, C. Hettich, K. Mølmer, E. S. Polzik, *Phys. Rev. Lett.* **2006**, *97*, 083604.
[15] H. Takahashi, K. Wakui, S. Suzuki, M. Takeoka, K. Hayasaka, A. Furusawa, M. Sasaki, *Phys. Rev. Lett.* **2008**, *101*, 233605.
[16] T. Gerrits, S. Glancy, T. S. Clement, B. Calkins, A. E. Lita, A. J. Miller, A. L. Migdall, S. W. Nam, R. P. Mirin, E. Knill, *Phys. Rev. A* **2010**, *82*, 031802(R).
[17] P. van Loock, *Laser Photonics Rev.* **2011**, *5*, 167.
[18] U. L. Andersen, J. S. Neergaard-Nielsen, P. van Loock, A. Furusawa, *Nat. Phys.* **2015**, *11*, 713.
[19] H. Do, R. Malaney, J. Green, *Quantum Eng.* **2021**, *3*, 60.
[20] D. Han, F. Sun, N. Wang, Y. Xiang, M. Wang, M. Tian, Q. He, X. Su, *Laser Photonics Rev.* **2023**, *17*, 2300103.
[21] M. Zhang, H. Kang, M. Wang, F. Xu, X. Su, K. Peng, *Photonics Res.* **2021**, *9*, 887.
[22] K. Huang, H. Le Jeannic, J. Ruaudel, V. B. Verma, M. D. Shaw, F. Marsili, S. W. Nam, E Wu, H. Zeng, Y.-C. Jeong, R. Filip, O. Morin, J. Laurat, *Phys. Rev. Lett.* **2015**, *115*, 023602.
[23] A. Ourjoumtsev, H. Jeong, R. Tualle-Brouri, P. Grangier, *Nature* **2007**, *448*, 784.
[24] J. Etesse, M. Bouillard, B. Kanseri, R. Tualle-Brouri, *Phys. Rev. Lett.* **2015**, *114*, 193602.
[25] D. V. Sychev, A. E. Ulanov, A. A. Pushkina, M. W. Richards, I. A. Fedorov, A. I. Lvovsky, *Nat. Photonics* **2017**, *11*, 379.
[26] M. Wang, M. Zhang, Z. Qin, Q. Zhang, L. Zeng, X. Su, C. Xie, K. Peng, *Laser Photonics Rev.* **2022**, *16*, 2200336.
[27] A. Serafini, S. De Siena, F. Illuminati, M. G. A. Paris, *J. Opt. B: Quantum Semiclass. Opt.* **2004**, *6*, S591.
[28] H. Le Jeannic, A. Cavaillès, K. Huang, R. Filip, J. Laurat, *Phys. Rev. Lett.* **2018**, *120*, 073603.
[29] N. Lee, H. Benichi, Y. Takeno, S. Takeda, J. Webb, E. Huntington, A. Furusawa, *Science* **2011**, *332*, 330.
[30] J. S. Neergaard-Nielsen, Y. Eto, C.-W. Lee, H. Jeong, M. Sasaki, *Nat. Photonics* **2013**, *7*, 439.
[31] H. Jeong, A. Zavatta, M. Kang, S.-W. Lee, L. S. Costanzo, S. Grandi, T. C. Ralph, M. Bellini, *Nat. Photonics* **2014**, *8*, 564.

 © 2024 Wiley-VCH GmbH

18638899, 0, Downloaded from https://onlinelibrary.wiley.com/doi/10.1002/lpor.202400174 by Shanxi University, Wiley Online Library on [14/10/2024]. See the Terms and Conditions (https://onlinelibrary.wiley.com/terms-and-conditions) on Wiley Online Library for rules of use; OA articles are governed by the applicable Creative Commons License

[32] O. Morin, K. Huang, J. Liu, H. L. Jeannic, C. Fabre, J. Laurat, *Nat. Photonics* **2014**, *8*, 570.
[33] A. E. Ulanov, D. Sychev, A. A. Pushkina, I. A. Fedorov, A. I. Lvovsky, *Phys. Rev. Lett.* **2017**, *118*, 160501.
[34] D. V. Sychev, A. E. Ulanov, E. S. Tiunov, A. A. Pushkina, A. Kuzhamuratov, V. Novikov, A. I. Lvovsky, *Nat. Commun.* **2018**, *9*, 3672.
[35] A. Tipsmark, R. Dong, A. Laghaout, P. Marek, M. Ježek, U. L. Andersen, *Phys. Rev. A* **2011**, *84*, 050301(R).
[36] B. Xia, J. Huang, H. Li, H. Wang, G. Zeng, *Nat. Commun.* **2023**, *14*, 1021.
[37] K. Liu, C. Cai, J. Li, L. Ma, H. Sun, J. Gao, *Appl. Phys. Lett.* **2018**, *113*, 261103.
[38] Y. Zhang, Z. Zhang, L. Liu, Y. Zhao, *Photonics* **2023**, *10*, 341.
[39] M. P. J. Lavery, F. C. Speirits, S. M. Barnett, M. J. Padgett, *Science* **2013**, *341*, 537.
[40] V. D'Ambrosio, N. Spagnolo, L. Del Re, S. Slussarenko, Y. Li, L. C. Kwek, L. Marrucci, S. P. Walborn, L. Aolita, F. Sciarrino, *Nat. Commun.* **2013**, *4*, 2432.
[41] H. Markus, B. Frédéric, F. Robert, *Phys. Rev. Lett.* **2021**, *127*, 263601.
[42] W. Zhang J. Gao, D. Zhang, Y. He, T. Xu, R. Fickler, L. Chen, *Phys. Rev. Appl.* **2018**, *10*, 044014.
[43] R. Fickler, R. Lapkiewicz, W. N. Plick, M. Krenn, C. Schaeff, S. Ramelow, A. Zeilinger, *Science* **2012**, *338*, 640.
[44] A. Mair, A. Vaziri, G. Weihs, A. Zeilinger, *Nature (London)* **2001**, *412*, 313.
[45] M. Malik, M. Erhard, M. Huber, M. Krenn, R. Fickler, A. Zeilinger, *Nat. Photonics* **2016**, *10*, 248.
[46] H. Cao, S.-C. Cao, C. Zhang, J. Wang, D.-Y. He, B.-H. Liu, Z.-W. Zhou, Y.-J. Chen, Z.-H. Li, S.-Y. Yu, J. Romero, Y.-F. Huang, C.-F. Li, G.-C. Guo, *Optica* **2020**, *7*, 232.
[47] R. Qu, Y. Wang, X. Zhang, S. Ru, F. Wang, H. Gao, F. Li, P. Zhang, *Optica* **2022**, *9*, 473.
[48] A. M. Marino, V. Boyer, R. C. Pooser, P. D. Lett, K. Lemons, K. M. Jones, *Phys. Rev. Lett.* **2008**, *101*, 093602.
[49] M. Lassen, G. Leuchs, U. L. Andersen, *Phys. Rev. Lett.* **2009**, *102*, 163602.
[50] A. Pecoraro, F. Cardano, L. Marrucci, A. Porzio, *Phys. Rev. A* **2019**, *100*, 012321.
[51] X. Pan, S. Yu, Y. Zhou, K. Zhang, K. Zhang, S. Lv, S. Li, W. Wang, J. Jing, *Phys. Rev. Lett.* **2019**, *123*, 070506.
[52] K. Liu, J. Guo, C. Cai, S. Guo, J. Gao, *Phys. Rev. Lett.* **2014**, *113*, 170501.
[53] S. Li, X. Pan, Y. Ren, H. Liu, S. Yu, J. Jing, *Phys. Rev. Lett.* **2020**, *124*, 083605.
[54] K. Zhang, S. Liu, Y. Chen, X. Wang, J. Jing, *Photonics Insights* **2022**, *1*, R06.
[55] L. Zeng, R. Ma, H. Wen, M. Wang, J. Liu, Z. Qin, X. Su, *Photonics Res.* **2022**, *10*, 777.
[56] R. Chen, H. Zhou, M. Moretti, X. Wang, J. Li, *IEEE Commun. Surv. Tut.* **2020**, *22*, 840.
[57] X.-L. Wang, X.-D. Cai, Z.-E. Su, M.-C. Chen, D. Wu, L. Li, N.-L. Liu, C.-Y. Lu, J.-W. Pan, *Nature (London)* **2015**, *518*, 516.
[58] S. Liu, Y. Lou, J. Jing, *Nat. Commun.* **2020**, *11*, 3875.
[59] S. Liu, Y. Lv, X. Wang, J. Wang, Y. Lou, J. Jing, *Phys. Rev. Lett.* **2024**, *132*, 100801.
[60] Y. Chen, S. Liu, Y. Lou, J. Jing, *Phys. Rev. Lett.* **2021**, *127*, 093601.
[61] Y. Ren, X. Wang, Y. Lv, D. Bacco, J. Jing, *Laser Photonics Rev.* **2022**, *16*, 2100586.
[62] S. Yu, K. Zhang, Y. Lou, S. Liu, J. Jing, *Laser Photonics Rev.* **2023**, *17*, 2201005.
[63] D.-S. Ding, W. Zhang, Z.-Y. Zhou, S. Shi, G.-Y. Xiang, X.-S. Wang, Y.-K. Jiang, B.-S. Shi, G.-C. Guo, *Phys. Rev. Lett.* **2015**, *114*, 050502.
[64] Y. Chen, J. Gao, J. Han, Z. Yuan, R. Li, Y. Jiang, J. Song, *Phys. Rev. A* **2023**, *108*, 022613.
[65] S.-L. Liu, Q. Zhou, S.-K. Liu, Y. Li, Y.-H. Li, Z.-Y. Zhou, G.-C. Guo, B.-S. Shi, *Commun. Phys.* **2019**, *2*, 75.
[66] L. Allen, M. W. Beijersbergen, R. J. C. Spreeuw, J. P. Woerdman, *Phys. Rev. A* **1992**, *45*, 8185.
[67] A. M. Yao, M. J. Padgett, *Adv. Opt. Photonics* **2011**, *3*, 161.
[68] Y.-H. Ye, L. Zeng, M.-X. Dong, W.-H. Zhang, E.-Z. Li, D.-C. Li, G.-C. Guo, D.-S. Ding, B.-S. Shi, *Phys. Rev. Lett.* **2022**, *129*, 193601.
[69] E. Karimi, B. Piccirillo, L. Marrucci, E Santamato, *Opt. Lett.* **2009**, *34*, 1225.
[70] E. Karimi, G. Zito, B. Piccirillo, L. Marrucci, E. Santamato, *Opt. Lett.* **2007**, *32*, 3053.
[71] A. I. Lvovsky, M. G. Raymer, *Rev. Mod. Phys.* **2009**, *81*, 299.
[72] P. Vaity, J. Banerji, R. P. Singh, *Phys. Lett. A* **2013**, *377*, 1154.
[73] A. Pecoraro, F. Cardano, L. Marrucci, A. Porzio, *Phys. Lett. A* **2024**, *500*, 129363.

© 2024 Wiley-VCH GmbH

18638899, 0, Downloaded from https://onlinelibrary.wiley.com/doi/10.1002/lpor.202400174 by Shanxi University, Wiley Online Library on [14/10/2024]. See the Terms and Conditions (https://onlinelibrary.wiley.com/terms-and-conditions) on Wiley Online Library for rules of use; OA articles are governed by the applicable Creative Commons License